HHS Public Access

Author manuscript

J Physiol. Author manuscript; available in PMC 2023 February 01.

Published in final edited form as:

J Physiol. 2022 February ; 600(3): 655–670. doi:10.1113/JP281415.

Intrauterine growth restriction elevates circulating acylcarnitines and suppresses fatty acid metabolism genes in the fetal sheep heart

Rachel R. Drake[1,2], **Samantha Louey**[1], **Kent L. Thornburg**[1,2]

[1]Center for Developmental Health, Knight Cardiovascular Institute, School of Medicine, Oregon Health and Science University, Portland, Oregon, USA

[2]Department of Chemical Physiology and Biochemistry, School of Medicine, Oregon Health and Science University, Portland, Oregon, USA

Abstract

At birth, the mammalian myocardium switches from using carbohydrates as the primary energy substrate to free fatty acids as the primary fuel. Thus, a compromised switch could jeopardize normal heart function in the neonate. Placental embolization in sheep is a reliable model of intrauterine growth restriction (IUGR). It leads to suppression of both proliferation and terminal differentiation of cardiomyocytes. We hypothesized that the expression of genes regulating cardiac fatty acid metabolism would be similarly suppressed in IUGR, leading to compromised processing of lipids. Following 10 days of umbilicoplacental embolization in fetal sheep, IUGR fetuses had elevated circulating long-chain fatty acylcarnitines compared with controls (C14: CTRL 0.012 ± 0.005 nmol/ml *vs*. IUGR 0.018 ± 0.005 nmol/ml, $P < 0.05$; C18: CTRL 0.027 ± 0.009 nmol/mol *vs*. IUGR 0.043 ± 0.024 nmol/mol, $P < 0.05$, $n = 12$ control, $n = 12$ IUGR) indicative of impaired fatty acid metabolism. Uptake studies using fluorescently tagged BODIPY-C12-saturated free fatty acid in live, isolated cardiomyocytes showed lipid droplet area and number were not different between control and IUGR cells. mRNA levels of sarcolemmal fatty acid transporters (CD36, FATP6), acylation enzymes (ACSL1, ACSL3), mitochondrial transporter (CPT1), β-oxidation enzymes (LCAD, HADH, ACAT1), tricarboxylic acid cycle enzyme (IDH), esterification enzymes (PAP, DGAT) and regulator of the lipid droplet formation (BSCL2) gene were all suppressed

Corresponding author: Kent Thornburg: Centre for Developmental Health, Knight Cardiovascular Institute, School of Medicine, Oregon Health and Science University, Portland, OR, USA. thornbur@ohsu.edu.

Author contributions

R.D. and K.T. designed the study. R.D. and S.L. performed the *in vivo* experiments and collected post mortem tissues. R.D. performed molecular and imaging experiments. R.D., S.L. and K.T. analysed the data. R.D. drafted the manuscript and K.T. and S.L. provided critical revisions. All authors approved the final version of the manuscript and agree to be accountable for all aspects of the work. R.D., S.L. and K.T. all qualify for authorship and all those who qualify are listed as authors.

Competing interests

The authors declare no conflicts of interest.

Supporting information

Additional supporting information can be found online in the Supporting Information section at the end of the HTML view of the article. Supporting information files available:

Peer Review History

Statistical Summary Document

The peer review history is available in the supporting information section of this article (https://doi.org/10.1113/JP281415#support-information-section).

in IUGR myocardium ($P < 0.05$). However, protein levels for these regulatory genes were not different between groups. This discordance between mRNA and protein levels in the stressed myocardium suggests an adaptive protection of key myocardial enzymes under conditions of placental insufficiency.

Graphical Abstarct

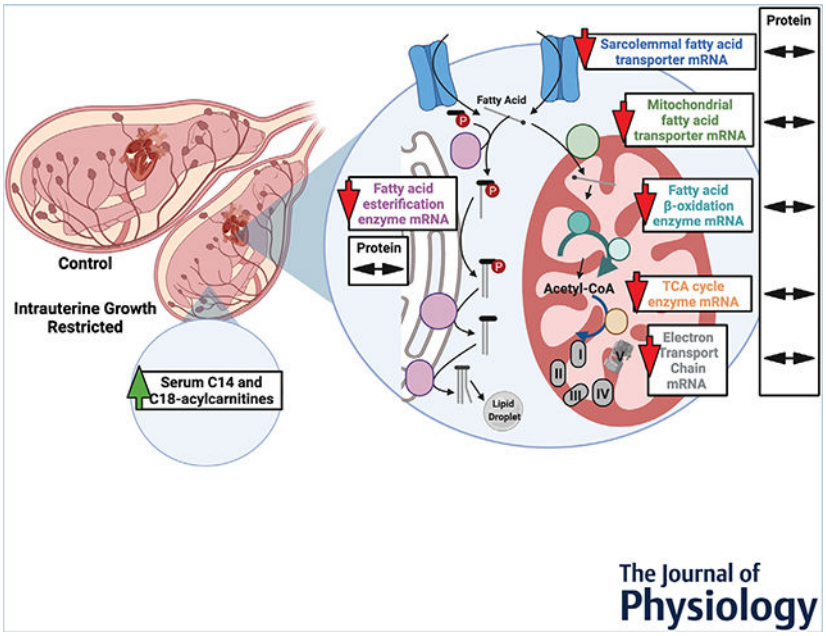

We investigated the degree to which the cardiac genes that regulate fatty acid metabolism were altered in growth-restricted fetuses compared with those that grew normally. As shown by the red arrows, messenger RNA levels for the genes studied were suppressed compared with controls. However, the double-headed arrows show that protein levels were unaffected. Circulating long-chain fatty acylcarnitines in the fetus were elevated, suggesting incomplete metabolism of free fatty acids. Whether these experimental conditions portend adverse outcomes in the postnatal period as the heart transitions to fatty acid metabolism requires further study.

Keywords

fetal heart; intrauterine growth restriction; lipid metabolism; placental insufficiency

Introduction

Placental insufficiency suppresses fetal growth, causing intrauterine growth restriction (IUGR) and is the second most common cause of perinatal mortality (Nardozza et al. 2017). In addition to being a common and complex perinatal problem, IUGR predisposes the fetus to a myriad of adult-onset diseases including cardiovascular and metabolic disease (Hoffman et al. 2017).

Various animal models have been used to investigate molecular responses to IUGR in the fetus. Sheep models are particularly advantageous as sheep are born precocial and have a similar organ development timeline (relative to gestational age) to humans (Morrison et al. 2018). The fetal heart is relatively protected from the detrimental effects of acute and chronic hypoxaemia because of its powerful vasodilatory capacity leading to a redistribution of cardiac output to the heart (Block et al. 1990; Gagnon et al. 1996; Poudel et al. 2015) and preservation of blood flow to the myocardium (Kiserud et al. 2000). Despite these protections, the heart is not fully protected from the effects of fetal hypoxaemia and restricted growth. Several sheep models of IUGR reveal physiological insights regarding the fetal cardiac response to placental insufficiency (Darby et al. 2020b): the models consistently report decreased cell cycle activity and binucleation, indicators of cell cycle activity, and maturation (Bubb et al. 2007; Louey et al. 2007; Morrison et al. 2007; Jonker et al. 2018).

The mammalian fetal heart utilizes primarily lactate and glucose (Fisher et al. 1980; Werner & Sicard, 1987; Lopaschuk & Jaswal, 2010) as fuels for energy production and the newborn heart utilizes primarily fatty acids (Werner et al. 1989; Bartelds et al. 2000, 2004). This dramatic switch is made around the time of birth. Presumably, the expression of the genes that code for the proteins required for fatty acid metabolism should be elevated in the fetal myocardium in preparation for augmented postnatal fatty acid oxidation when fat-laden milk becomes available. However, the temporal regulation of the genes required for the fatty acid metabolism switch in normal and IUGR development are poorly understood. Components of these pathways have been previously investigated in sheep (Botting et al. 2018; Davies et al. 2020; Darby et al. 2020a) but there remains an incomplete understanding.

Few studies have investigated oxidative metabolism in the fetal heart in response to IUGR. In one model of IUGR, pregnant ewes exposed to elevated ambient temperatures develop placental insufficiency and have impaired oxidative metabolism in fetal skeletal muscle and liver (Brown et al. 2015). However, since blood flow to fetal skeletal muscle and liver is known to be compromised in IUGR compared with the heart, it is uncertain whether this metabolic alteration occurs in myocardium. Barry et al. (2016) found that the myocardium in fetuses compromised by IUGR is more sensitive to insulin, suggesting that placental insufficiency can modify metabolic processes in the fetal heart. Most recently, Dimasi et al. (2021) used two-photon imaging in the caruncletomy model of IUGR and reported reduced redox ratios in the IUGR fetal heart. They conclude that this may be due to an increased reliance on glycolysis for ATP production as a reduced redox ratio is suggestive of augmented glycolysis. This could be secondary to impaired oxidative metabolism. However, the fatty acid metabolic responses of fetal cardiomyocytes to conditions of chronic hypoxaemia have been understudied. Hypoxaemia is a hallmark of IUGR and has been shown to inhibit fatty acid β-oxidation and induces lipid droplet accumulation in hepatocellular carcinoma cells (Mylonis et al. 2019).

The aim of this study was to determine the effect of placental insufficiency on fatty acid metabolism in the near-term fetal heart. We measured circulating acylcarnitines (a marker for impaired fatty acid oxidation), lipid droplet formation and storage using a fluorescent tagged fatty acid molecule, BODIPY-C12, and the expression levels of genes and proteins

required for the switch from glycolysis to β-oxidation in the myocardium of IUGR fetuses. We hypothesized that circulating acylcarnitines would be elevated, lipid droplets would be larger and gene and protein expression of fatty acid metabolic machinery would be suppressed in IUGR myocardium.

Methods

Ethical approval

All protocols in the present study were carried out according to guidelines laid down by Oregon Health and Science University's (OHSU) Institutional Animal Care and Use Committee (approval number IP 566) which is in compliance with the Animal Welfare Act and Public Health Service. It is accredited by the American Association for Accreditation of Laboratory Animal Care.

Animals

Twenty time-bred ewes of mixed western breeds were purchased from a commercial supplier and brought to the laboratory 4–7 days before surgery for acclimatization. All protocols were approved by the Institutional Animal Care and Use Committee. A total of 38 fetuses were studied; included were 34 twins (from 17 pregnancies), two triplets from the same pregnancy and two singletons. The study groups included a balance of males and females. See Table 1 for details.

Surgery

Ewes were fasted for 24 h prior to surgery with water *ad libitum.* Induction of anaesthesia was with intravenous diazepam (10 mg) and ketamine (400 mg) followed by immediate intubation. Anaesthesia was maintained with 1–2% isoflurane in a 70:30 mixture of oxygen:nitrous oxide during mechanical ventilation. Sterile surgery was performed at 110 ± 2 days gestational age (d GA, term ≈147 d GA), as previously described (Louey et al. 2007). In brief, a midline incision was made through the ewe's linea alba to access the uterus and the fetal rump was exteriorized though a uterine incision. A catheter (1.8 mm OD polyvinyl; Scientific Commodities, V-8, Lake Havasu City, AZ, USA) was inserted 7 cm into the fetal femoral artery for blood pressure measurements, sampling and microsphere injections. Catheter tip position was 1–2 cm below the renal arteries and above the umbilical arteries, confirmed at autopsy. Prior to returning the fetus to the uterus, a catheter (1.8 mm OD) was sutured to the rump for delivery of antibiotics and measurement of amniotic pressure. The uterus was sutured securely to prevent fluid loss. Following instrumentation of the first fetus, its twin was exposed through a second incision in the uterus and catheterized in the aforementioned manner. Penicillin G (1,000,000 units per fetus; Bristol-Myers Squibb, Princeton, NJ, USA) and ciprofloxacin (2 mg/fetus) was injected into the amniotic space of each fetus through their respective amniotic catheters. All catheters were then flushed with heparinized saline. The exteriorized ends of the catheters were securely tied off, exteriorized through a flank incision in the ewe and finally secured to a pouch sutured to the ewe's flank. The midline was closed in anatomical layers. Following surgery, isoflurane administration was stopped and the endotracheal tube removed once the ewe had autonomous respiratory drive. Ewes were given 0.3 mg Buprenex (bupreneorphine HCl),

and 0.05 mg/kg sustained release buprenorphine (ZooPharm, CO) subcutaneously at the conclusion of surgery, according to the veterinary practices at OHSU. Ewes were returned to a clean pen and monitored. A minimum of 3 days' recovery period was given to ewes prior to commencing experiments. Ewes were provided with feed and water *ad libitum* throughout the recovery and experimental period.

Experimental protocol

Two groups of fetuses were studied: one group was subjected to 10 days of umbilicoplacental embolization (UPE; this is the IUGR group) and the other was their age-matched controls. For fetuses in the IUGR groups, 20–50 μm (mean ± SD diameter, 35 ± 9 μm) non-radioactive, non-soluble microspheres (Sephadex Superfine G-25; Amersham, Sweden; 1% w/v suspended in heparinized saline with 0.02% Tween 80) were injected into the fetal femoral artery catheter to reduce P_{aO2} by approximately 8 mmHg from baseline values on study day 1 as previously reported (Louey et al. 2007).

Studies for all fetuses commenced at 114–117 d GA and were terminated at 124–127 d GA. Included in the study were 17 ewes carrying twins where both twins were included, one ewe carrying triplets of which two fetuses were included, and two singletons. Fetuses were randomly assigned to each experimental group; one control and one experimental fetus per ewe if the ewe was carrying multiple fetuses. During the experimental time period, ewes were kept in individual stanchions with water and food *ad libitum.* Arterial blood samples were taken from all fetuses to assess pH, glucose and blood gas status using a blood gas analyser (Radiometer ABL825, OH).

Plasma acylcarnitine assays

Arterial blood samples were collected on the final day of the study (following 10 days of UPE) at 126 ± 1 d GA from a subset of fetuses (n = 12 controls, n = 12 IUGR). Samples were heparinized and centrifuged for 10 min, 2500 g at 4°C and plasma stored at −20°C and analysed for acylcarnitines by electrospray tandem mass spectrometry (Applied Biosystems/MDS SCIEX API 3000) at the Biochemical Genetics Laboratory, Mayo Clinic (Smith & Matern, 2010). Samples were compared with known internal standards and were identified by characteristic mass-to-charge ratios.

Tissue collection

Ewes were euthanised with an intravenous overdose of sodium phenobarbital (SomnaSol, 80 mg/kg, Covetrus, OH, USA). As a result, the fetuses were deeply anaesthetized, exteriorized and given 10,000 units of heparin though the umbilical vein followed by 10 ml of saturated KCl to arrest the heart in diastole. The fetus was then removed from the uterus and weighed. The heart was excised, trimmed in a standardized manner and weighed. Brain and liver weights were documented.

Fourteen fetal hearts (seven control, seven experimental) were separated into left ventricle, right ventricle and septum, and each wall was snap-frozen in liquid nitrogen; only left ventricular tissue was used in this study. Of these hearts, 12 were used for qPCR (six control, six experimental). Western blotting was conducted on all 14 animals (seven control,

seven experimental) plus an additional nine animals (four control, five experimental) that each had a 5 mm^3 section of mid-wall left ventricle (LV) flash-frozen before dissociation to isolate cardiomyocytes for live-imaging studies; the cut edges of the left ventricle were sealed with SuperGlue and cardiomyocyte isolation was not compromised.

Cardiomyocyte isolation

Twenty-four hearts in total were dissociated for imaging (12 control, 12 IUGR). Of these, nine hearts (four control, five experimental) were also used for western blotting (see above). The aorta was perfused in a retrograde fashion using established methods in the laboratory (Louey et al. 2007). In brief, the heart was perfused with a warmed (39°C) and 95% oxygen/5% CO_2 gassed solution in the following order: (1) Ca^{2+}-free Tyrodes buffer (140 mM NaCl, 5 mM KCl, 1 mM $MgCl_2 \cdot 6H_2O$, 10 mM glucose, 10 mM Hepes; pH 7.35 with NaOH) for ~5–10 min, until the tissue was washed out, (2) Tyrodes buffer with enzymes (160 U/ml Type II Collagenase (Worthington Batch 46B16451), 0.78 U/ml Type XIV protease) (Sigma) until the heart was sufficiently digested (~5–10 min), and (3) KB solution (74 mM glutamic acid, 30 mM KCl, 30 mM KH_2PO_4, 20 mM taurine, 3 mM $MgSO_4$, 0.5 mM EGTA, 10 mM Hepes, 10 mM glucose; pH 7.37 with KOH). Following the KB perfusate rinse, the left ventricular free wall was dissected and gently agitated in a conical tube containing KB solution to release cardiomyocytes. The cell slurry was left to rest at room temperature for 30–45 min before imaging. A 140 μl aliquot of left ventricular cells (~250 k cell/ml) were used for live imaging.

BODIPY-C_{12} fluorescent fatty acid live imaging

A protocol, established in our lab for studying placental explants (Kolahi et al. 2016), was adapted for fetal cardiomyocytes to track the incorporation of an exogenous long-chain saturated fatty acid into lipid droplets. BODIPY-FL-C_{12} (Molecular Probes, cat#D3822) is a 12-carbon chain-length saturated fatty acid linked to the fluorophore BODIPY (4,4-difluoro-3a,4a-diaza-s-indacene) (Stahl et al. 1999; Wang et al. 2010; Kassan et al. 2013; Rambold et al. 2015; Kolahi et al. 2016).

The BODIPY-C_{12} conjugate biologically resembles an 18-carbon saturated fatty acid and permits tracking of exogenous supplied fatty acid via the BODIPY fluorophore which is an intensely fluorescent, intrinsically lipophilic molecule. The 10 μM solutions of BODIPY-FL C_{12} were prepared by diluting a 2.5 mM stock solution in DMSO 1:250 in fetal KB solution (KB supplemented with 2 mM glutamine, 200 μM sodium pyruvate, 2 mM lactate, 1 mM glucose) supplemented with 0.1% fatty acid-free bovine serum albumin and incubated for 30 min (37°C, in the dark) to allow fatty acid:BSA conjugation.

Cells were incubated in KB in eight-well μ-slides (Idibi, cat#80821) with 2 μM of BODIPY-C_{12} for 60 min (39°C) and imaged using the 63× oil lens on the Zeiss 880 LSM with Airyscan. Z-stack images were collected after 60 min. BODIPY was imaged with a 488 laser (intensity 0.6, gain 825, digital gain 1.0). Some 90–130 slices, 0.2 μm thick were acquired per frame (18–26 μm thickness, 3–18 frames per animal).

Image analysis

Z-stacks were processed (Airyscan) and maximum intensity projections performed in ZEN Black Software (Zeiss). Fiji software was used to analyse all images obtained. Images were enhanced using Enhance Local Contrast (CLAHE: blocksize = 9, histogram = 256, maximum = 4), despeckled and background subtracted (rolling = five). Lipid droplet particles were analysed by filtering for the following parameters: circularity (0.8–1), size (0.0314 <minimal detectable size for LSM880> to 3 <maximum intracardiomyocyte lipid droplet size (Wang et al. 2013a)>, AutoThreshold (Intermodes dark) and images were converted to a mask for lipid droplets and entire cells.

We measured the average individual lipid droplet size (lipid droplet area, μm^2), the area occupied by lipid droplets relative to total cell area (lipid droplet area/total cell area), and number of lipid droplets relative to cell area (lipid droplet number/total cell area).

For each animal, 13–56 cells were measured in 4–12 frames. Masks were manually verified to ensure the parameters did not accidentally exclude or include an unintentional measurement from a non-viable cell.

RNA isolation and gene expression

RNA was isolated as previously described (Lindgren et al. 2019) from 40 to 50 μg of left ventricular myocardium using Trizol, a steel bead and TissueLyser LT (Qiagen, Germantown, MD, USA), 50 oscillations/s for 3 min. Isolates were further purified using RNeasy Mini Columns (Qiagen). Reverse transcription on 1 μg RNA was conducted to synthesize cDNA using the High-Capacity cDNA Reverse Transcription Kit (ABI) and diluted 1:20 prior to PCR. Quantitative PCR was carried out using SYBR Green in the Stratagene Mx3005. Primers are listed in Table 2. Gene expression was analysed using the ΔC_t method. Genes of interest were normalized to housekeeping gene ribosomal protein L37a (RPL37a), which was not altered by umbilicoplacental embolization.

Western blotting

We did not have working antibodies for all proteins in sheep. Thus, for several enzymes and transporters we have mRNA levels but not protein levels. Protein was isolated as previously described (Lindgren et al. 2019). In brief, 20–30 μg of left ventricular myocardium using RIPA lysis buffer (MilliporeSigma) with a Complete Mini Protease 227 Inhibitor tablet (MilliporeSigma) and phosphatase inhibitor cocktails I and II (MilliporeSigma). Tissue was added to chilled lysis buffer in 2 ml tubes containing a stainless-steel bead and lysed (4 min, 50 Hz TissueLyser LT). Protein was quantified by a standard bicinchoninic acid assay as routinely performed in our lab (Jonker et al. 2015) and diluted to a uniform concentration across all groups (2 $\mu g/\mu l$). Gels were poured (stacking: 4% acrylamide; resolving: 12% acrylamide) using SureCast Stacking Buffer and Resolving Buffer along with SureCast system (Invitrogen). Fifteen micrograms of protein was loaded with 6x dye (10% betamercaptoethanol) and separated by SDS-PAGE (90 min, 100 mV, BioRad system) with running buffer (24.8 mM Tris, 191.8 mM glycine, 3.5 mM SDS). Protein was transferred to PVDF membranes (MilliporeSigma) with transfer buffer (24.8 mM Tris, 191.8

mM glycine), and blocked (5% milk in Tris-buffered saline + 0.01% Tween 20 (TBST), 1 h, room temperature).

Antibody incubations took place in the following order: (1) primary antibody (4°C, overnight), (2) TBST rinses (3 × 10 min), and (3) secondary antibody (room temperature, 1 h), all on a rocker. Dilutions and antibodies can be found in Table 3.

SuperSignal West Dura chemiluminscence substrate was used to visualize membranes (ThermoFisher Scientific). GBOX (SynGene) and GeneSys software (version 4.3.7.0) were used to image and analyse the blots. Band intensities were expressed as area under the curve, normalized against alpha-tubulin, GAPDH or total protein (as determined by Ponceau S staining immediately after protein transfer, prior to primary antibody incubation) which was not affected by IUGR.

Statistics

Unpaired Student's *t* tests with *post hoc* Bonferroni correction were used to test for differences between end P_{aO2}, glucose, body weight, heart:body weight, brain:liver, acylcarnitine levels, lipid droplet sizes, gene and protein levels. All generated datasets and analysis for the present study are available from the corresponding author upon request. All data were analysed using GraphPad Prism 6 and are presented as means ± SD unless noted otherwise. *P* values < 0.05 were considered statistically significant, denoted with an asterisk.

Results

Arterial blood

IUGR fetuses were hypoxaemic (10-day average P_{aO2}: IUGR 13.3 ± 0.7 mmHg *vs.* control 20.8 ± 1.9 mmHg, $P < 0.0001$) and hypoglycaemic (10-day average: IUGR 0.9 ± 0.1 mM *vs.* control 1.1 ± 0.2 mM, $P = 0.0002$) during UPE (Fig. 1A, B). This led to fetuses that were 28% lighter than controls (Fig. 1C, $P < 0.0001$), and although they were asymmetrically growth-restricted (Fig. 1E), heart weight/body weight was not different between groups (Fig. 1D, $P = 0.695$).

Circulating plasma acylcarnitines are higher in intrauterine growth-restricted fetuses

Elevated plasma acylcarnitines are indicative of incomplete partial fatty acid oxidation. In these studies, free carnitine levels were not different between groups (Fig. 2A). Long-chain fatty acid-C14 and -C18 plasma acylcarnitines were elevated in growth-restricted fetuses compared with control (Fig. 2B, D). C16 (palmitate)-acylcarnitine was not different between groups (Fig. 2C).

BODIPY-C12 long-chain fatty acid uptake and lipid droplet formation

Lipid droplet size (Fig. 3A), area occupied by lipid droplets relative to cell area (Fig. 3B), and number of lipid droplets (Fig. 3C) were not different in IUGR cardiomyocytes compared with control. A representative image of BODIPY-C12 lipid droplet formation in control and IUGR cardiomyocytes is shown in Fig. 3D.

Sarcolemmal fatty acid transporter expression

Sarcolemmal lipid transporter genes CD36 and FATP6 both had lower mRNA levels in IUGR myocardium compared with controls, with FATP6 expression being especially suppressed (Fig. 4A, B). CD36 protein levels in IUGR hearts were not different from controls (Fig. 4C).

Fatty acid acylation enzyme expression

Acyl-CoA synthetase (ACSL) is responsible for the acylation and activation of fatty acids upon entry to the cell. The ACSL1 isoform gene (Fig. 5A) and protein (Fig. 5C) levels were not different between control and IUGR myocardium, while ACSL3 mRNA was suppressed in IUGR myocardium (Fig. 5B.

Mitochondrial transporter expression

The expression of the CPT1 gene, the rate-limiting protein in mitochondrial utilization of fatty acids was significantly lower in growth-restricted hearts (Fig. 6A). The myocardium expresses both CPT1a (fetal isoform) and CPT1b (adult isoform) and the protein levels for both were not different between groups (Fig. 6B, C). Voltage-dependent anion channel protein (VDAC), which transports other mitochondrial metabolites was not different between IUGR and control myocardium (Fig. 6D).

β-Oxidation enzyme expression

mRNA levels of mitochondrial β-oxidation enzymes LCAD, HADH and ACAT1 were all lower in myocardium from IUGR fetuses relative to controls (Figs 7A, C, and D) while VLCAD was not different. Protein levels of LCAD, the only enzyme in this group for which we had a working antibody, were not different between the groups (Fig. 7E).

Tricarboxylic acid (TCA) cycle enzyme expression

Myocardial mRNA expression of isocitrate dehydrogenase (IDH), a TCA cycle enzyme that catalyses the production of the first reducing equivalent (NADH) was suppressed in IUGR myocardium (Fig. 8A). The first step of the TCA cycle which joins oxaloacetate and acetyl-CoA to form citrate is performed by citrate synthase; protein levels for citrate synthase were not different between control and IUGR (Fig. 8B).

Electron transport chain subunit expression

The electron transport chain is composed of five complexes, each with several subunits. Protein expression for the five subunits (NDUFB8 (CI), SDHB (CII), UQCRC2 (CIII), MTCO1 (CIV) nor ATP5A(CV)) were not different between groups (Fig. 9). Figure 9F shows a representative blot for all complexes included in the antibody cocktail. mRNA levels were not measured.

Fatty acid esterification enzyme expression

Glycerol phosphate acyltransferase (GPAT) catalyses the first step of fatty-acyl-CoA esterification by adding fatty-acyl-CoA to glycerol-3-phosphate. Phosphatidic acid phosphatase (PAP) is responsible for converting phosphatidic acid to diacylglycerol (DAG),

and diacylglycerol acyltransferase (DGAT) converts DAG into triacylglycerol (TAG) by adding a third fatty-acyl group to the glycerol backbone. BSCL2 (Seipin) is associated with lipid droplet morphogenesis and may aid in anchoring lipid droplets to the endoplasmic reticulum. Gene expression for all except GPAT is suppressed in IUGR myocardium (Fig. 10).

Glycolysis and β-oxidation regulator expression

Since our gene expression data suggest a suppression of fatty acid transport and oxidation, we sought to determine whether this might lead to increased activity of the glycolytic pathway. Pyruvate dehydrogenase kinase (PDK4) is a well-established gatekeeper of the carbon flux from glycolysis to the TCA cycle. It accomplishes this through phosphorylation and inhibition of pyruvate dehydrogenase, the final step of glycolysis. Amounts of the PDK4 gene were not different between IUGR and control (Fig. 11).

Discussion

We tested the hypothesis that the metabolic systems responsible for fatty acid handling would be suppressed in IUGR fetal hearts compared with control. We hypothesized that circulating acylcarnitines would be elevated in fetal plasma and that intracellular droplets from exogenous lipids would be larger in cardiomyocytes from growth-restricted fetuses. We found higher levels of circulating long-chain fatty acylcarnitines in IUGR fetuses, indicative of global impaired fatty acid oxidation. Fatty acid transporters, esterification and metabolic machinery all had lower gene expression in IUGR myocardium with the exception of acylation enzyme ACSL1 and esterification enzyme GPAT. Despite widespread suppression of mRNA expression, none of the key fatty acid enzyme or transporter products were altered in IUGR myocardium. Lipid droplet formation was not different in isolated IUGR cardiomyocytes compared with control.

In the perinatal period, it is normal for acylcarnitines to be elevated as newborns transition to a high-fat diet (Vieira Neto et al. 2012). However, IUGR infants have even higher circulating long-chain acylcarnitines relative to normal birthweight controls (El-Wahed et al. 2017). Consistent with these clinical data, we found elevated long-chain circulating acylcarnitines (C14 and C18) in IUGR fetuses. However, we did not measure the difference in concentrations of acylcarnitines in arterial *vs*. venous blood in the coronary sinus. Thus, we cannot be sure of the degree to which the elevation in acylcarnitines is dominated by the heart. However, because the heart is a major organ preparing to use free fatty acids as a primary fuel, we speculate that it is a major contributor to the circulating concentrations of acylcarnitines under conditions of placental insufficiency. Regardless, elevated acylcarnitines are still indicative of impaired fatty acid metabolism within the fetal compartment and are another indicator of dysregulated metabolism in the stressed fetus. This could impact the transition from a low-lipid environment *in utero* to a lipid-rich environment postnatally. If the metabolic deficiency persists, this could portend problems beyond the suckling period. Additionally, if the fetus is metabolically disadvantaged as it transitions to fatty acid metabolism, it may be ill-equipped to adapt to fuelling the increased workload in response to haemodynamic changes at birth and lead to long-term poor health.

Elevated long-chain acylcarnitines are also indicative of adverse outcomes in chronic heart failure patients (Ahmad et al. 2016). Interestingly, Beauchamp et al. (2015) noted elevated total acylcarnitines in adult mice born IUGR, pointing to persistent impairments in metabolism that were set in the fetus but are associated with increased heart failure risk in adulthood.

Our hypothesis that cardiomyocyte lipid droplets would be altered in IUGR fetal cardiomyocytes, as they are in conditions of hypoxia, was not supported by our experimental data. There was no difference in lipid droplet size in IUGR fetal cardiomyocytes compared with control. Lipid droplet size is a downstream measure of fatty acid esterification in the endoplasmic reticulum and relies on GPAT, PAP and DGAT. This suggests that although there was a significant suppression of genes responsible for fatty acid esterification and lipid droplet formation, this did not result in a functional difference in lipid storage. It is possible that the suppressed mRNA levels did not lead to a suppression of protein levels for these enzymes. Unfortunately, we did not have antibodies that work in sheep to test this. Another possibility is that esterification enzyme function was not altered in IUGR hearts. However, additional functional measures including enzyme activity of GPAT, PAP and DGAT would be required to further explore this possibility.

DGAT is responsible for the final conversion of diacylglycerol to triacylglycerol. A suppression of DGAT enzyme activity (as found in our study) should lead to an elevation in myocardial diacylglycerols and lower triacylglycerols. This is consistent with higher diacylglycerols and lower triacylglycerols in fetal baboon myocardium exposed to *in utero* maternal undernutrition (Muralimanoharan et al. 2017). Persistently suppressed DGAT could set the scene for elevated myocardial diacylglycerols as seen in failing human hearts (Chokshi et al. 2012).

Gene expression of critical components in mitochondrial β-oxidation and fatty acid esterification was suppressed in IUGR myocardium. ACSL is known to play a role in determining the fate of fatty-acyl CoAs, with ACSL1 and ACSL3 being the predominant isoforms in the heart. ACSL1 colocalizes to mitochondria and when deficient, leads to an impairment of fatty acid oxidation (Ellis et al. 2011). ACSL3 is important for esterification, as its knockdown blocks lipid accumulation when endoplasmic reticulum-stress is present (Chang et al. 2011). Suppression of ACSL3 but not ACSL1 suggests an impairment of fatty acid activation destined for the endoplasmic reticulum but not the mitochondrion. This implies that fatty acid trafficking to the endoplasmic reticulum might be impaired while trafficking to the mitochondrion is maintained. The suppression of endoplasmic reticulum-associated ACSL3 in our study suggests a mechanism that may stifle the normal transition to fatty acid storage at birth. This may not be critical before birth, but if these changes persist, the newborn heart would be unprepared to handle the high levels of circulating lipids after birth.

We were surprised to find that for all of the genes studied, protein levels were unchanged. This apparent protective mechanism fits with other physiological responses suggesting a favoured status for the fetal heart under stressful conditions. For example, under acute reductions in fetal arterial oxygen content, blood flow to the heart, brain and adrenal glands

is conserved compared with other organs (Cohn et al. 1974; Giussani, 2016; Darby et al. 2020b). This leads to asymmetrical growth with an increase in the head-to-abdomen (or brain-to-liver) ratio; fetuses facing placental insufficiency in our study showed a similar response. We have previously shown that reduced oxygen content in fetal arterial blood leads to astonishing levels of coronary vasodilation under the influence of nitric oxide and adenosine (Thornburg & Reller, 1999). Additionally, fatty acid oxidation proteins are preferentially preserved in the fetal alligator heart in response to hypoxia (Alderman et al. 2019). Although the expression of genes regulating fatty acid metabolism were considerably suppressed, it is reasonable to suggest that the cellular levels of the protein products of these genes are protected under stressful conditions to maintain an organ vital to the survival of the fetus. A mismatch has also been reported in a maternal undernutrition mouse model of IUGR where there were no differences in mitochondrial electron transport chain proteins despite a suppression of fatty acid oxidation in adult offspring myocardium (Beauchamp et al. 2015). Similar lasting metabolic effects have also been shown in the hearts of IUGR guinea pigs (Botting et al. 2018). Although little is known about the long-term fatty acid metabolic effects in sheep models, perturbations in cardiac glucose metabolic pathways persist in low birthweight lambs (Wang et al. 2013b).

Maternal nutrient restriction and maternal hypoxia in guinea pigs increases CD36 and FATP6, and decreases acyl-CoA carboxylase (the first step in fatty acid synthesis) but does not alter ACADL, ACADVL or CPT1b gene expression in adult offspring (Botting et al. 2018). Our present study found suppression of all of these genes in fetal IUGR myocardium with the exception of no significant difference in ACADVL gene expression. It is possible that the increased availability of fatty acid postnatally alone induces increased mitochondrial fatty acid transporter expression (Xiao *et al.,* 2001) in these guinea pigs, but this study did not determine whether the intracardiomyocyte fatty acid handling machinery is equipped to handle this presumed influx in fatty acids. Since there is a mismatch in sarcolemmal gene expression and oxidation and fatty acid synthesis gene expression, it is possible that this could lead to a disruption in the balance between fatty acid uptake and intracellular processes including oxidation and storage.

Placental insufficiency leads to both nutritional and hypoxic stresses and similar conditions are found in humans (Morrison, 2008). Little is known about the impact of these suboptimal intrauterine conditions on the fetus's ability to successfully metabolically transition to *ex utero* life. During this transition to extrauterine life, cardiomyocytes normally lose their proliferative capacity (Jonker et al. 2015) and IUGR cardiomyocytes have premature suppression of proliferation and maturation (Louey et al. 2007; Jonker et al. 2018). These studies indicated that the fetal heart is sensitive to placental insufficiency.

There is evidence for a metabolic influence on cardiomyocyte maturation and cell-cycle arrest in human organoids (Mills et al. 2017). Changes in cardiomyocyte proliferation and maturation are well characterized in the perinatal period and in IUGR, but less is known about perinatal changes in cardiomyocyte metabolism even in healthy fetuses and even less is known about this process in IUGR fetal cardiomyocytes. A perinatal rise in cortisol is thought to play a role in organ maturation with regard to both cell-cycle activity and metabolic maturation. Cortisol stimulates cell-cycle activity in control fetal sheep hearts

(Giraud et al. 2006). A recent paper similarly shows that dexamethasone upregulates fatty acid oxidation and mRNA expression of fatty acid oxidation components including CD36, CPT1a, CPT1b and LCAD (Ivy et al. 2021). Cortisol is increased in IUGR, but interestingly cell-cycle activity (Louey et al. 2007) and mRNA levels of these fatty acid metabolism components are suppressed. A rise in cortisol is expected to stimulate cell-cycle activity and fatty acid metabolic maturation in controls, but in IUGR these pathways are suppressed. An in-depth study interrogating the interconnectedness of cardiomyocyte maturation and fatty acid metabolic maturation between normal development, IUGR and cortisol is warranted.

In summary, placental embolization causes IUGR and suppresses myocardial fatty acid transport and metabolism genes. Unexpectedly, lower mRNA levels of metabolic genes in the heart did not translate to a corresponding reduction in protein levels. Also, lipid droplet formation was not different. The underlying reason for the mismatch between genes, proteins and function is not known, but the increase in circulating acylcarnitines implies a bourgeoning metabolic dysfunction. Though the fetal heart does not rely on fatty acid metabolism, this metabolic ability is critical post-natally. The degree to which the observed suppression of fatty acid metabolism genes persists postnatally, or whether this gene suppression translates to functional protein changes is not known. We also know that these impairments in gene expression do not impact immediate survival afterbirth (Louey et al. 2000) or survival to young adulthood under resting conditions (Louey et al. 2005). It remains to be seen how cardiac metabolism and function are compromised under secondary postnatal stress.

Supplementary Material

Refer to Web version on PubMed Central for supplementary material.

Acknowledgements

The authors thank the OHSU Advanced Light Microscopy Core (Stefanie Kaech Petrie, Crystal Chaw and Aurelie Snyder) for technical assistance with the imaging studies, Dietrich Matern (Biochemical Genetics Laboratory, Mayo Clinic) and Melanie Gillingham (Oregon Health and Science University) for conducting the acylcarnitine assays. A tremendous amount of gratitude goes to Cindy McEvoy, George Giraud and Melanie Gillingham for consulting on the project.

Funding

This research was supported by the National Heart, Lung and Blood Institute (R01 HL146997) and the Eunice Kennedy Shriver National Institute of Child Health and Human Development (Grant P01 HD034430-20). American Heart Association Predoctoral Fellowship (19PRE34380190, 01/2019-03/2019). R.R.D. is supported by the Eunice Kennedy Shriver National Institute of Child Health and Human Development National Research Service Award Fellowship (Grant F30 HD096812).

Biography

Rachel Drake received her BSc in Biochemistry at the University of Minnesota and is currently pursuing her MD/PhD at Oregon Health and Science University. She completed her PhD with Kent Thornburg and is now finishing medical school. She plans to pursue a residency in paediatrics. Her research and clinical interests are in neonatal metabolism and nutrition.

Data availability statement

All data supporting the results are present in the manuscript and in the statistical summary document.

References

Abudurexiti M, Zhu W, Wang Y, Wang J, Xu W, Huang Y, Zhu Y, Shi G, Zhang H, Zhu Y, Shen Y, Dai B, Wan F, Lin G & Ye D (2020). Targeting CPT1B as a potential therapeutic strategy in castration-resistant and enzalutamide-resistant prostate cancer. Prostate 80, 950–961. [PubMed: 32648618]

Ahmad T, Kelly JP, McGarrah RW, Hellkamp AS, Fiuzat M, Testani JM, Wang TS, Verma A, Samsky MD, Donahue MP, Ilkayeva OR, Bowles DE, Patel CB, Milano CA, Rogers JG, Felker GM, O'Connor CM, Shah SH & Kraus WE (2016). Prognostic implications of long-chain acylcarnitines in heart failure and reversibility with mechanical circulatory support. J Am Coll Cardiol 67, 291–299. [PubMed: 26796394]

Alderman SL, Crossley DA, Elsey RM & Gillis TE (2019). Hypoxia-induced reprogramming of the cardiac phenotype in American alligators (*Alligator mississippiensis*) revealed by quantitative proteomics. Sci Rep 9, 8592. [PubMed: 31197188]

Barker DJ, Gelow J, Thornburg K, Osmond C, Kajantie E, & Eriksson JG (2010). The early origins of chronic heart failure: impaired placental growth and initiation of insulin resistance in childhood. Eur J Heart Fail 12, 819–825. [PubMed: 20504866]

Barry JS, Rozance PJ, Brown LD, Anthony RV, Thornburg KL & Hay WW Jr (2016). Increased foetal myocardial sensitivity to insulin-stimulated glucose metabolism during ovine fetal growth restriction. Exp Biol Med (Maywood) 241, 839–847. [PubMed: 26873920]

Bartelds B, Knoester H, Smid GB, Takens J, Visser GH, Penninga L, van der Leij FR, Beaufort-Krol GC, Zijlstra WG, Heymans HS & Kuipers JR (2000). Perinatal changes in myocardial metabolism in lambs. Circulation 102, 926–931. [PubMed: 10952964]

Bartelds B, Takens J, Smid GB, Zammit VA, Prip-Buus C, Kuipers JR & van der Leij FR (2004). Myocardial carnitine palmitoyltransferase I expression and long-chain fatty acid oxidation in fetal and newborn lambs. Am J Physiol Heart Circ Physiol 286, H2243–H2248. [PubMed: 14751860]

Beauchamp B, Thrush AB, Quizi J, Antoun G, McIntosh N, Al-Dirbashi OY, Patti ME & Harper ME (2015). Undernutrition during pregnancy in mice leads to dysfunctional cardiac muscle respiration in adult offspring. Biosci Rep 35, e00200. [PubMed: 26182362]

Block BS, Schlafer DH, Wentworth RA, Kreitzer LA & Nathanielsz PW (1990). Regional blood flow distribution in fetal sheep with intrauterine growth retardation produced by decreased umbilical placental perfusion. J Dev Physiol 13, 81–85. [PubMed: 2283464]

Botting KJ, Loke XY, Zhang S, Andersen JB, Nyengaard JR & Morrison JL (2018). IUGR decreases cardiomyocyte endowment and alters cardiac metabolism in a sex- and cause-of-IUGR-specific manner. Am J Physiol Regul Integr Comp Physiol 315, R48–R67. [PubMed: 29561647]

Brown LD, Rozance PJ, Bruce JL, Friedman JE, Hay WW Jr. & Wesolowski SR (2015). Limited capacity for glucose oxidation in fetal sheep with intrauterine growth restriction. Am J Physiol Regul Integr Comp Physiol 309, R920–R928. [PubMed: 26224688]

Bubb KJ, Cock ML, Black MJ, Dodic M, Boon WM, Parkington HC, Harding R & Tare M (2007). Intrauterine growth restriction delays cardiomyocyte maturation and alters coronary artery function in the fetal sheep. J Physiol 578, 871–881. [PubMed: 17124269]

Chang YS, Tsai CT, Huangfu CA, Huang WY, Lei HY, Lin CF, Su IJ, Chang WT, Wu PH, Chen YT, Hung JH, Young KC & Lai MD (2011). ACSL3 and GSK-3beta are essential for lipid upregulation induced by endoplasmic reticulum stress in liver cells. J Cell Biochem 112, 881–893. [PubMed: 21328461]

Chokshi A, Drosatos K, Cheema FH, Ji R, Khawaja T, Yu S, Kato T, Khan R, Takayama H, Knoll R, Milting H, Chung CS, Jorde U, Naka Y, Mancini DM, Goldberg IJ & Schulze PC (2012). Ventricular assist device implantation corrects myocardial lipotoxicity, reverses insulin resistance, and normalizes cardiac metabolism in patients with advanced heart failure. Circulation 125, 2844–2853. [PubMed: 22586279]

Cohn HE, Sacks EJ, Heymann MA & Rudolph AM (1974). Cardiovascular responses to hypoxemia and acidemia in fetal lambs. Am J Obstet Gynecol 120, 817–824. [PubMed: 4429091]

Darby JRT, Sorvina A, Bader CA, Lock MC, Soo JY, Holman SL, Seed M, Kuchel T, Brooks DA, Plush SE & Morrison JL (2020a). Detecting metabolic differences in fetal and adult sheep adipose and skeletal muscle tissues. J Biophotonics 13, e201960085. [PubMed: 31793184]

Darby JRT, Varcoe TJ, Orgeig S & Morrison JL (2020b). Cardiorespiratory consequences of intrauterine growth restriction: influence of timing, severity and duration of hypoxaemia. Theriogenology 150, 84–95. [PubMed: 32088029]

Davies KL, Camm EJ, Atkinson EV, Lopez T, Forhead AJ, Murray AJ & Fowden AL (2020). Development and thyroid hormone dependence of skeletal muscle mitochondrial function towards birth. J Physiol 598, 2453–2468. [PubMed: 32087026]

Dimasi CG, Lazniewska J, Plush SE, Saini BS, Holman SL, Cho SKS, Wiese MD, Sorvina A, Macgowan CK, Seed M, Brooks DA, Morrison JL & Darby JRT (2021). Redox ratio in the left ventricle of the growth restricted fetus is positively correlated with cardiac output. J Biophotonics, e202100157. [PubMed: 34499415]

El-Wahed MAA, El-Farghali OG, ElAbd HSA, El-Desouky ED & Hassan SM (2017). Metabolic derangements in IUGR neonates detected at birth using UPLC-MS. Egypt J Med Hum Genet 18, 281–287.

Ellis JM, Mentock SM, Depetrillo MA, Koves TR, Sen S, Watkins SM, Muoio DM, Cline GW, Taegtmeyer H, Shulman GI, Willis MS & Coleman RA (2011). Mouse cardiac acyl coenzyme a synthetase 1 deficiency impairs fatty acid oxidation and induces cardiac hypertrophy. Mol Cell Biol 31, 1252–1262. [PubMed: 21245374]

Fisher DJ, Heymann MA & Rudolph AM (1980). Myocardial oxygen and carbohydrate consumption in fetal lambs in utero and in adult sheep. Am J Physiol 238, H399–H405. [PubMed: 7369385]

Gagnon R, Johnston L & Murotsuki J (1996). Fetal placental embolization in the late-gestation ovine fetus: alterations in umbilical blood flow and fetal heart rate patterns. Am J Obstet Gynecol 175, 63–72. [PubMed: 8694077]

Giraud GD, Louey S, Jonker S, Schultz J & Thornburg KL (2006). Cortisol stimulates cell cycle activity in the cardiomyocyte of the sheep fetus. Endocrinology 147, 3643–3649. [PubMed: 16690807]

Giussani DA (2016). The fetal brain sparing response to hypoxia: physiological mechanisms. J Physiol 594, 1215–1230. [PubMed: 26496004]

Hoffman DJ, Reynolds RM & Hardy DB (2017). Developmental origins of health and disease: current knowledge and potential mechanisms. Nutr Rev 75, 951–970. [PubMed: 29186623]

Huang D, Li T, Li X, Zhang L, Sun L, He X, Zhong X, Jia D, Song L, Semenza GL, Gao P & Zhang H (2014). HIF-1-mediated suppression of acyl-CoA dehydrogenases and fatty acid oxidation is critical for cancer progression. Cell Rep 8, 1930–1942. [PubMed: 25242319]

Ivy JR, Carter RN, Zhao JF, Buckley C, Urquijo H, Rog-Zielinska EA, Panting E, Hrabalkova L, Nicholson C, Agnew EJ, Kemp MW, Morton NN, Stock SJ, Wyrwoll C, Ganley IG & Chapman KE (2021). Glucocorticoids regulate mitochondrial fatty acid oxidation in fetal cardiomyocytes. J Physiol 599, 4901–4924, Advance online publication. [PubMed: 34505639]

Jonker SS, Giraud MK, Giraud GD, Chattergoon NN, Louey S, Davis LE, Faber JJ, Thornburg KL (2010) Cardiomyocyte enlargement, proliferation and maturation during chronic fetal anaemia in sheep. Exp Physiol 95, 131–139. [PubMed: 19700519]

Jonker SS, Kamna D, LoTurco D, Kailey J & Brown LD (2018). IUGR impairs cardiomyocyte growth and maturation in fetal sheep. J Endocrinol 239, 253–265. [PubMed: 30143557]

Jonker SS, Louey S, Giraud GD, Thornburg KL & Faber JJ (2015). Timing of cardiomyocyte growth, maturation, and attrition in perinatal sheep. FASEB J 29, 4346–4357. [PubMed: 26139099]

Kassan A, Herms A, Fernandez-Vidal A, Bosch M, Schieber NL, Reddy BJ, Fajardo A, Gelabert-Baldrich M, Tebar F, Enrich C, Gross SP, Parton RG & Pol A (2013). Acyl-CoA synthetase 3 promotes lipid droplet biogenesis in ER microdomains. J Cell Biol 203, 985–1001. [PubMed: 24368806]

Kiserud T, Ozaki T, Nishina H, Rodeck C & Hanson MA (2000). Effect of NO, phenylephrine, and hypoxemia on ductus venosus diameter in fetal sheep. Am J Physiol Heart Circ Physiol 279, H1166–H1171. [PubMed: 10993780]

Kolahi K, Louey S, Varlamov O & Thornburg K (2016). Real-time tracking of BODIPY-C12 long-chain fatty acid in human term placenta reveals unique lipid dynamics in cytotrophoblast cells. PLoS One 11, e0153522. [PubMed: 27124483]

Li T, Li X, Meng H, Chen L & Meng F (2020). ACSL1 affects triglyceride levels through the PPARgamma pathway. Int J Med Sci 17, 720–727. [PubMed: 32218693]

Lindgren IM, Drake RR, Chattergoon NN & Thornburg KL (2019). Down-regulation of MEIS1 promotes the maturation of oxidative phosphorylation in perinatal cardiomyocytes. FASEB J 33, 7417–7426. [PubMed: 30884246]

Lopaschuk GD & Jaswal JS (2010). Energy metabolic phenotype of the cardiomyocyte during development, differentiation, and postnatal maturation. J Cardiovasc Pharmacol 56, 130–140. [PubMed: 20505524]

Louey S, Cock ML & Harding R (2005). Long term consequences of low birthweight on postnatal growth, adiposity and brain weight at maturity in sheep. J Reprod Dev 51, 59–68. [PubMed: 15750297]

Louey S, Cock ML, Stevenson KM & Harding R (2000). Placental insufficiency and fetal growth restriction lead to postnatal hypotension and altered postnatal growth in sheep. Pediatr Res 48, 808–814. [PubMed: 11102551]

Louey S, Jonker SS, Giraud GD & Thornburg KL (2007). Placental insufficiency decreases cell cycle activity and terminal maturation in fetal sheep cardiomyocytes. J Physiol 580, 639–648. [PubMed: 17234700]

Mills RJ, Titmarsh DM, Koenig X, Parker BL, Ryall JG, Quaife-Ryan GA, Voges HK, Hodson MP, Ferguson C, Drowley L, Plowright AT, Needham EJ, Wang QD, Gregorevic P, Xin M, Thomas WG, Parton RG, Nielsen LK, Launikonis BS, James DE, Elliott DA, Porrello ER & Hudson JE (2017). Functional screening in human cardiac organoids reveals a metabolic mechanism for cardiomyocyte cell cycle arrest. Proc Natl Acad Sci U S A 114, E8372–E8381. [PubMed: 28916735]

Morrison JL (2008). Sheep models of intrauterine growth restriction: fetal adaptations and consequences. Clin Exp Pharmacol Physiol 35, 730–743. [PubMed: 18498533]

Morrison JL, Berry MJ, Botting KJ, Darby JRT, Frasch MG, Gatford KL, Giussani DA, Gray CL, Harding R, Herrera EA, Kemp MW, Lock MC, McMillen IC, Moss TJ, Musk GC, Oliver MH, Regnault TRH, Roberts CT, Soo JY & Tellam RL (2018). Improving pregnancy outcomes in humans through studies in sheep. Am J Physiol Regul Integr Comp Physiol 315, R1123–R1153. [PubMed: 30325659]

Morrison JL, Botting KJ, Dyer JL, Williams SJ, Thornburg KL & McMillen IC (2007). Restriction of placental function alters heart development in the sheep fetus. Am J Physiol Regul Integr Comp Physiol 293, R306–R313. [PubMed: 17428893]

Muralimanoharan S, Li C, Nakayasu ES, Casey CP, Metz TO, Nathanielsz PW & Maloyan A (2017). Sexual dimorphism in the fetal cardiac response to maternal nutrient restriction. J Mol Cell Cardiol 108, 181–193. [PubMed: 28641979]

Mylonis I, Simos G & Paraskeva E (2019). Hypoxia-inducible factors and the regulation of lipid metabolism. Cells 8, 214.

Nardozza LM, Caetano AC, Zamarian AC, Mazzola JB, Silva CP, Marcal VM, Lobo TF, Peixoto AB & Araujo Junior E (2017). Fetal growth restriction: current knowledge. Arch Gynecol Obstet 295, 1061–1077. [PubMed: 28285426]

Poudel R, McMillen IC, Dunn SL, Zhang S & Morrison JL (2015). Impact of chronic hypoxemia on blood flow to the brain, heart, and adrenal gland in the late-gestation IUGR sheep fetus. Am J Physiol Regul Integr Comp Physiol 308, R151–R162. [PubMed: 25427766]

Rambold AS, Cohen S & Lippincott-Schwartz J (2015). Fatty acid trafficking in starved cells: regulation by lipid droplet lipolysis, autophagy, and mitochondrial fusion dynamics. Dev Cell 32, 678–692. [PubMed: 25752962]

Smith EH & Matern D (2010). Acylcarnitine analysis by tandem mass spectrometry. Curr Protoc Hum Genet Chapter 17, Unit 17 18 11–20.

Stahl A, Hirsch DJ, Gimeno RE, Punreddy S, Ge P, Watson N, Patel S, Kotler M, Raimondi A, Tartaglia LA & Lodish HF (1999). Identification of the major intestinal fatty acid transport protein. Mol Cell 4, 299–308. [PubMed: 10518211]

Thornburg KL & Reller MD (1999). Coronary flow regulation in the fetal sheep. Am J Physiol 277, R1249–R1260. [PubMed: 10564194]

Vieira Neto E, Fonseca AA, Almeida RF, Figueiredo MP, Porto MA & Ribeiro MG (2012). Analysis of acylcarnitine profiles in umbilical cord blood and during the early neonatal period by electrospray ionization tandem mass spectrometry. Braz J Med Biol Res 45, 546–556. [PubMed: 22488223]

Wang H, Lei M, Hsia RC & Sztalryd C (2013a). Analysis of lipid droplets in cardiac muscle. Methods Cell Biol 116, 129–149. [PubMed: 24099291]

Wang H, Wei E, Quiroga AD, Sun X, Touret N & Lehner R (2010). Altered lipid droplet dynamics in hepatocytes lacking triacylglycerol hydrolase expression. Mol Biol Cell 21, 1991–2000. [PubMed: 20410140]

Wang KC, Lim CH, McMillen IC, Duffield JA, Brooks DA & Morrison JL (2013b). Alteration of cardiac glucose metabolism in association to low birth weight: experimental evidence in lambs with left ventricular hypertrophy. Metabolism 62, 1662–1672. [PubMed: 23928106]

Werner JC & Sicard RE (1987). Lactate metabolism of isolated, perfused fetal, and newborn pig hearts. Pediatr Res 22, 552–556. [PubMed: 3684382]

Werner JC, Sicard RE & Schuler HG (1989). Palmitate oxidation by isolated working fetal and newborn pig hearts. Am J Physiol 256, E315–E321. [PubMed: 2919670]

Key points

- The fetal heart relies on carbohydrates *in utero* and must be prepared to metabolize fatty acids after birth but the effects of compromised fetal growth on the maturation of this metabolic system are unknown.
- Plasma fatty acylcarnitines are elevated in intrauterine growth-restricted (IUGR) fetuses compared with control fetuses, indicative of impaired fatty acid metabolism in fetal organs.
- Fatty acid uptake and storage are not different in IUGR cardiomyocytes compared with controls.
- mRNA levels of genes regulating fatty acid transporter and metabolic enzymes are suppressed in the IUGR myocardium compared with controls, while protein levels remain unchanged.
- Mismatches in gene and protein expression, and increased circulating fatty acylcarnitines may have long-term implications for offspring heart metabolism and adult health in IUGR individuals. This requires further investigation.

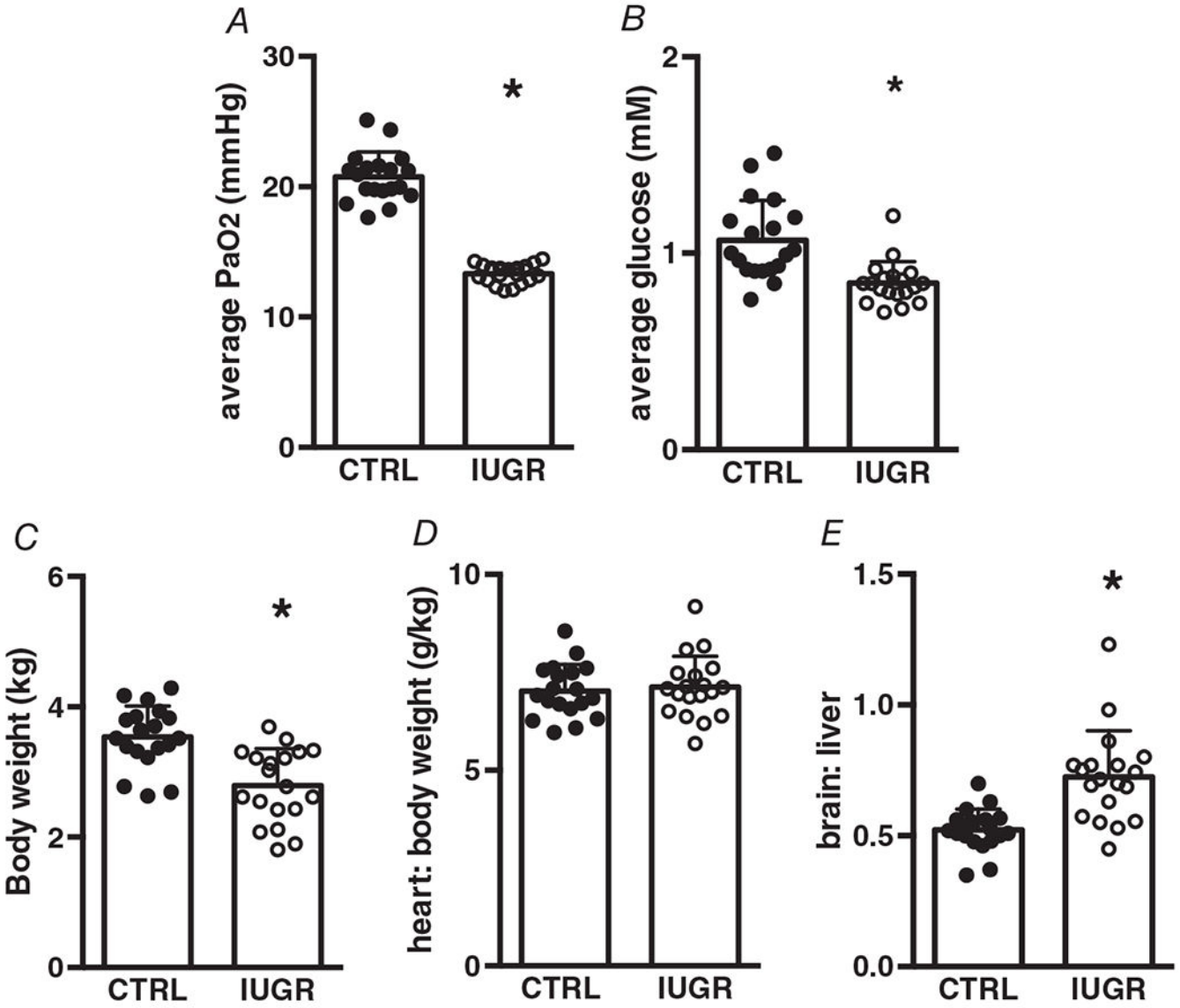

Figure 1. Umbilicoplacental embolization induces hypoxaemia, hypoglycaemia, and asymmetric growth restriction

A, hypoxaemia, $P < 0.0001$. *B,* hypoglycaemia, $P = 0.0002$. *C,* growth restriction (low body weight), $P < 0.0001$. *D,* no change in heart to body weight ratio, $P = 0.695$. *E,* asymmetric growth (increased brain-to-liver ratio), $P < 0.0001$. Average P_{aO2} and glucose reflect the 10-day average of each. $n = 19$ control, $n = 19$ IUGR. Means ± SD, $*P < 0.05$.

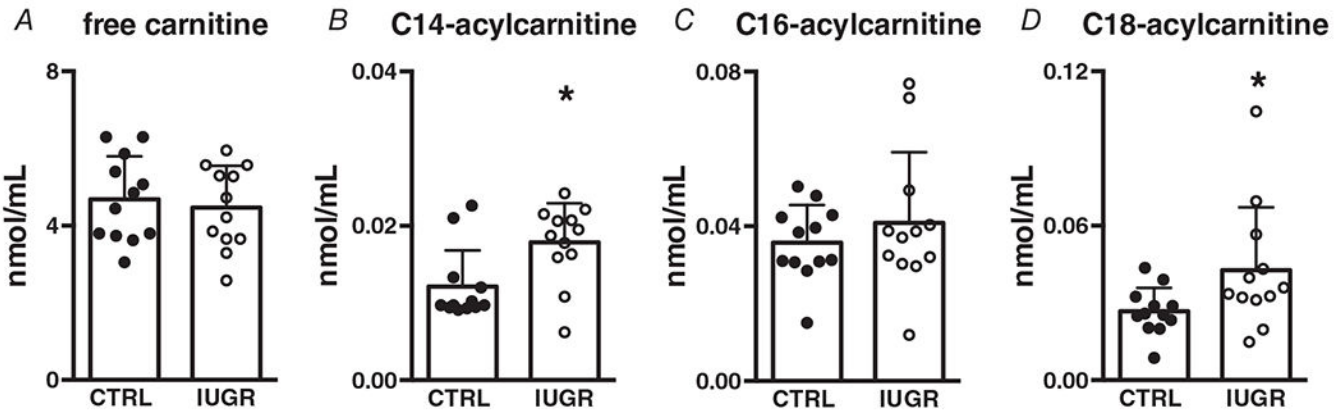

Figure 2. Intrauterine growth-restricted (IUGR) fetuses have elevated C14 and C18-acylcarnitine

A, no differences in free carnitine, $P = 0.635$ higher circulating long-chain. *B,* C14, $P = 0.009$. *D,* C18 fatty acylcarnitines, $P = 0.0443$ and no differences in *C*, C16 fatty acylcarnitines, $P = 0.397$. $n = 12$ control, $n = 12$ IUGR. Means ± SD, $^*P < 0.05$.

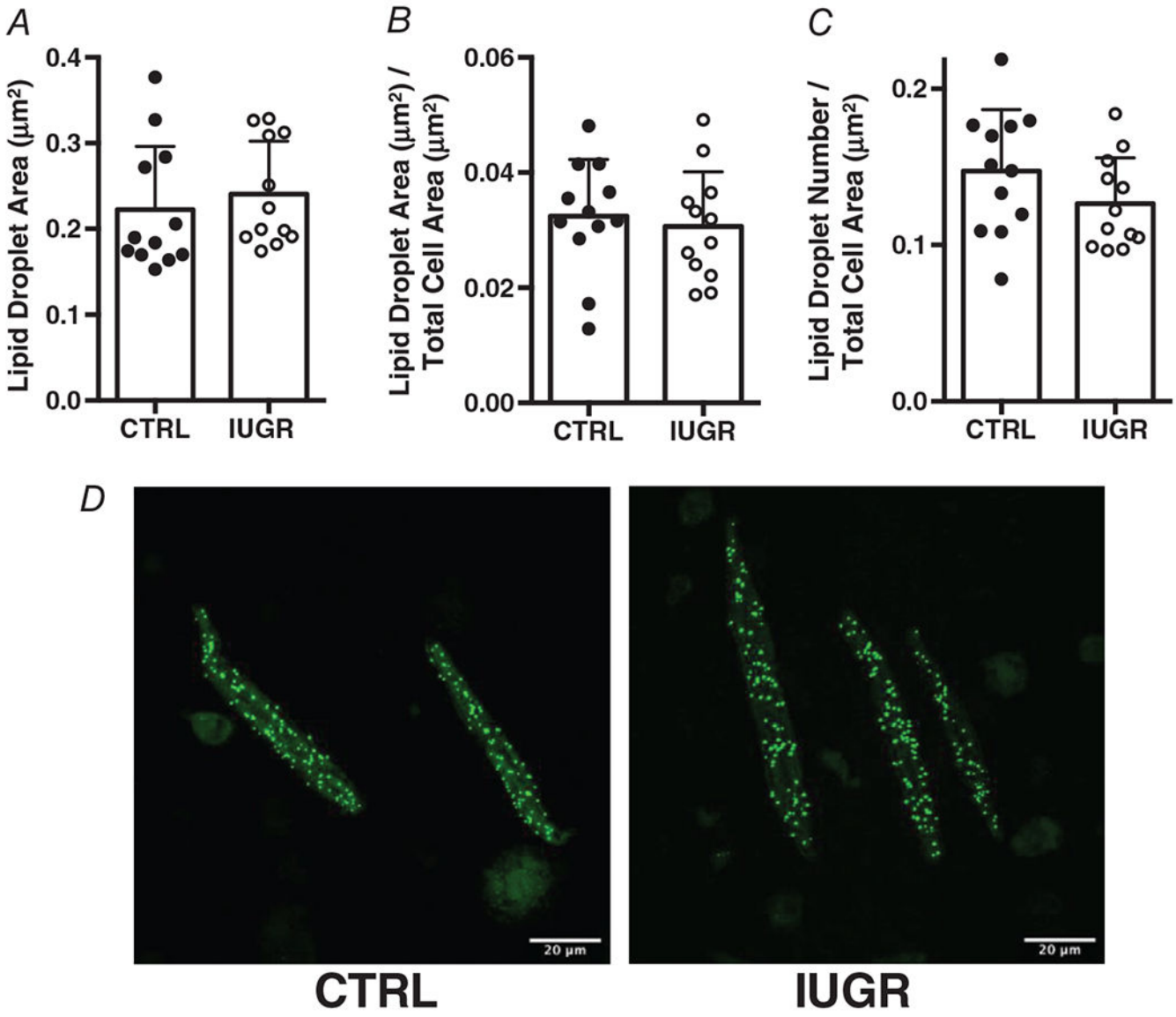

Figure 3. Intrauterine growth-restricted. (IUGR) and control cardiomyocytes do not differ in their formation of lipid droplets

A, lipid droplet size, $P = 0.521$. *B*, lipid droplet size relative to cell size, $P = 0.654$. *C*, number of lipid droplets relative to cell size, $P = 0.154$. $n = 12$ control, $n = 12$ IUGR. Means ± SD. *D*, Images are representative lipid droplets from control and IUGR heart.

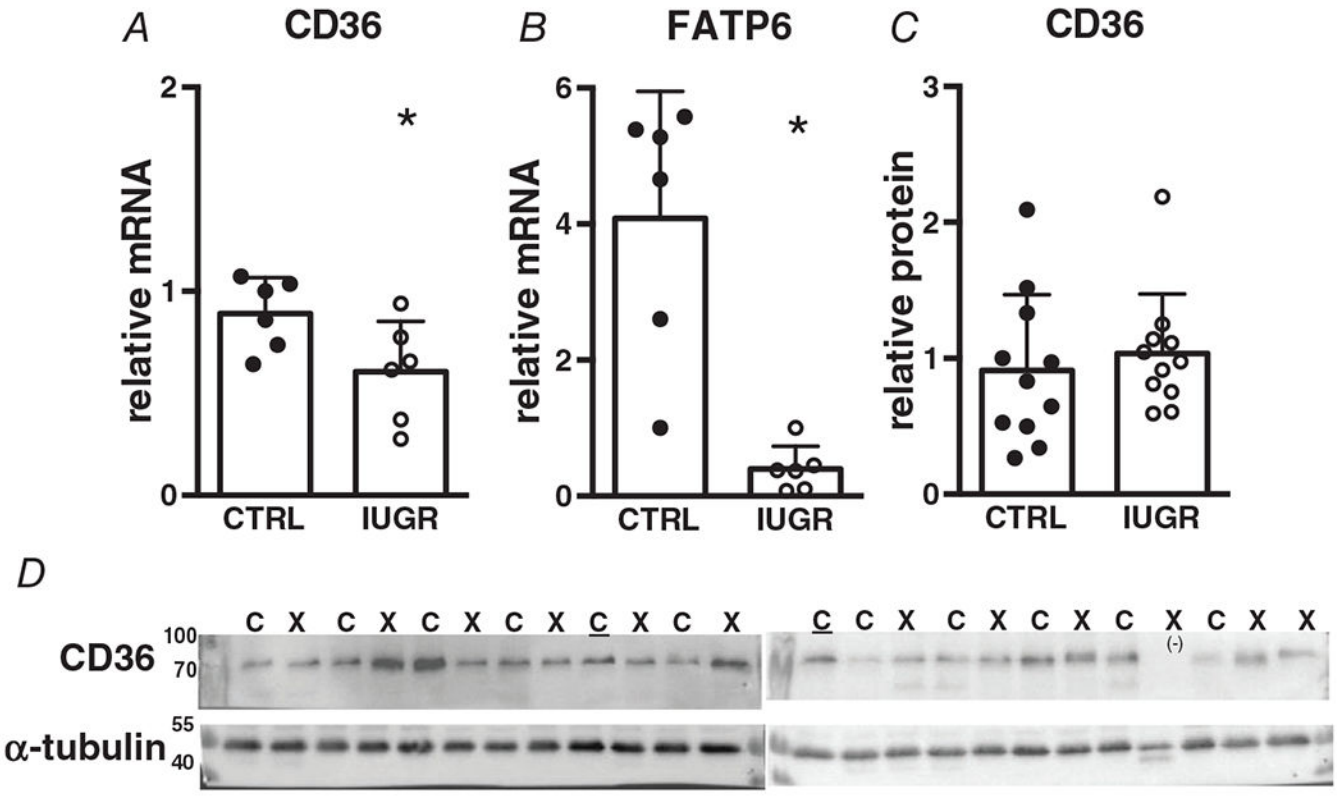

Figure 4. Gene (relative to RPL37a) and protein (relative to alpha-tubulin) expression of sarcolemmal fatty acid transporters in growth-restricted left ventricule myocardium

mRNA: $n = 6$ control, $n = 6$ IUGR (CD36 $P = 0.0435$, FATP $P = 0.0008$), protein: $n = 11$ control, $n = 11$ IUGR (CD36 $P = 0.569$). Means ± SD, $^*P < 0.05$. In *D*: C = Control, X = IUGR, C = Calibrator Control, (−) = excluded. Numbers adjacent to ladder represent kDa.

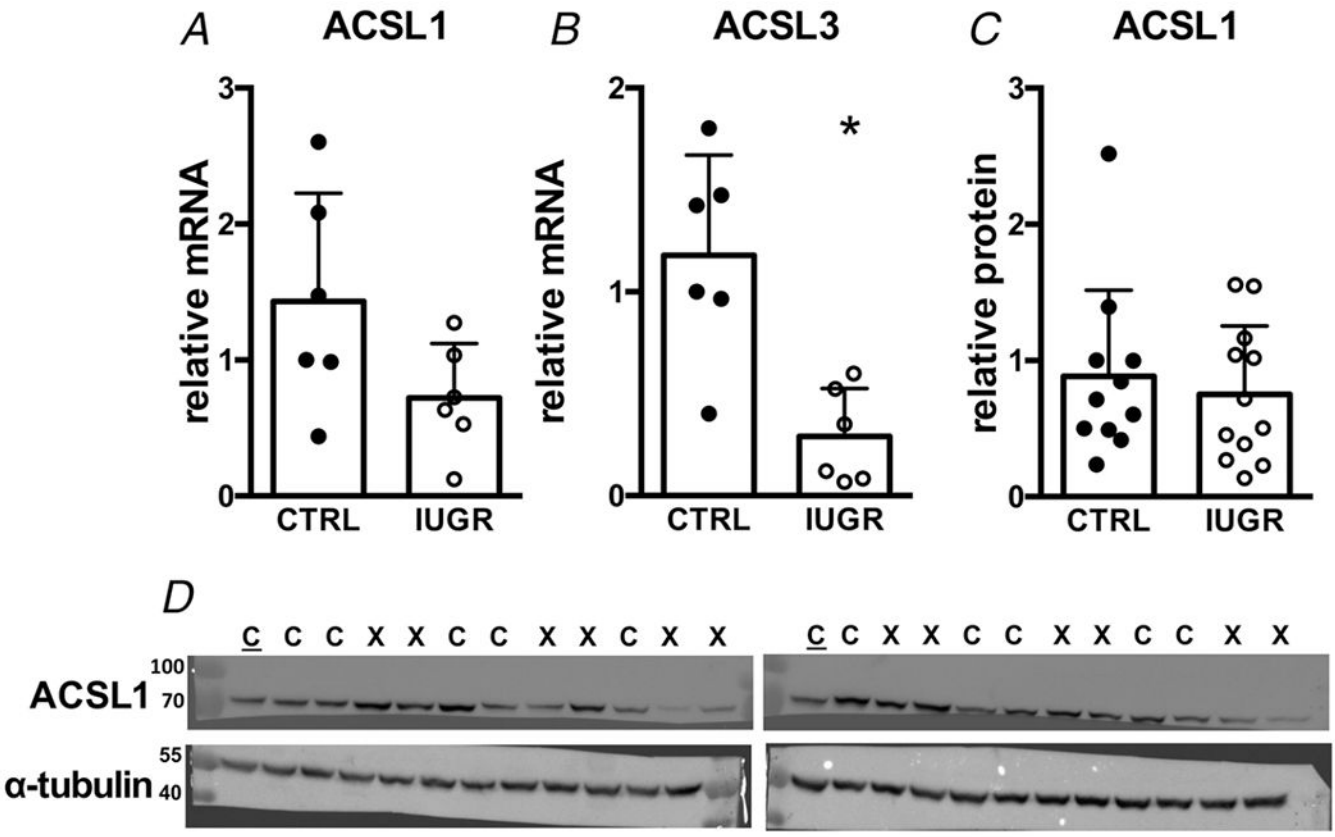

Figure 5. Gene (relative to RPL37a) and protein (relative to alpha-tubulin) expression of fatty acid activation enzymes in growth-restricted myocardium

mRNA: $n = 6$ control, $n = 6$ IUGR, (ACSL1 $P = 0.0795$, ACSL3 $P = 0.0026$). Protein: $n = 11$ control, $n = 12$ IUGR, (ACSL1 $P = 0.585$). Means ± SD, $^*P < 0.05$. In *D*: C = Control, X = IUGR, C = Calibrator Control. Numbers adjacent to ladder represent kDa.

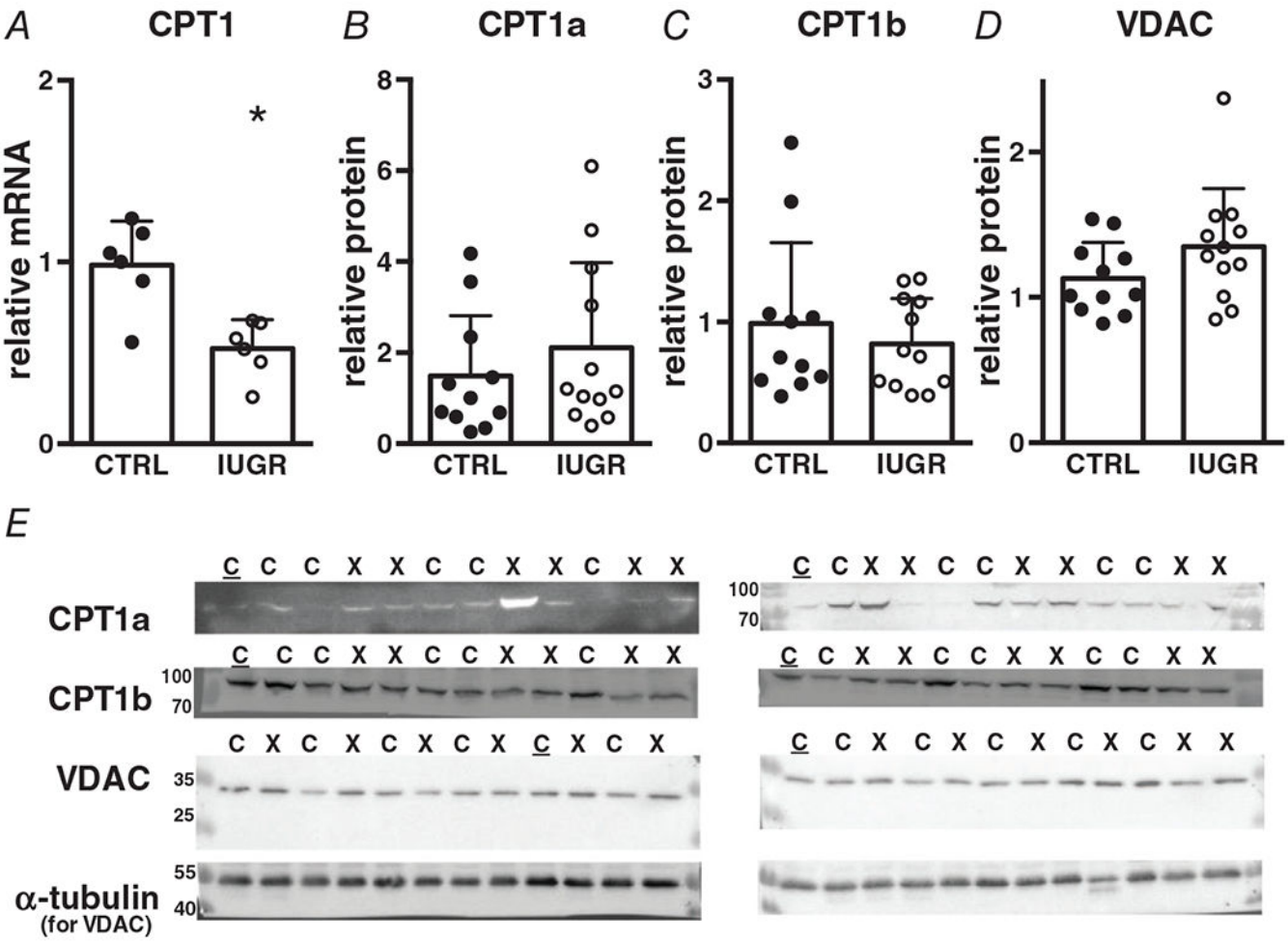

Figure 6. Gene (relative to RPL37a) and protein (relative to total protein or alpha-tubulin) expression of mitochondrial transporters in growth-restricted myocardium

mRNA: $n = 6$ control, $n = 6$ IUGR (CPT1 $P = 0.0029$), protein: $n = 11$ control, $n = 12$ IUGR (CPT1a $P = 0.375$, CPT1b $P = 0.462$, VDAC **P** = 0.134). Means ± SD, $*P < 0.05$. In *E*: C = Control, X = IUGR, C = Calibrator Control. Numbers adjacent to ladder represent kDa.

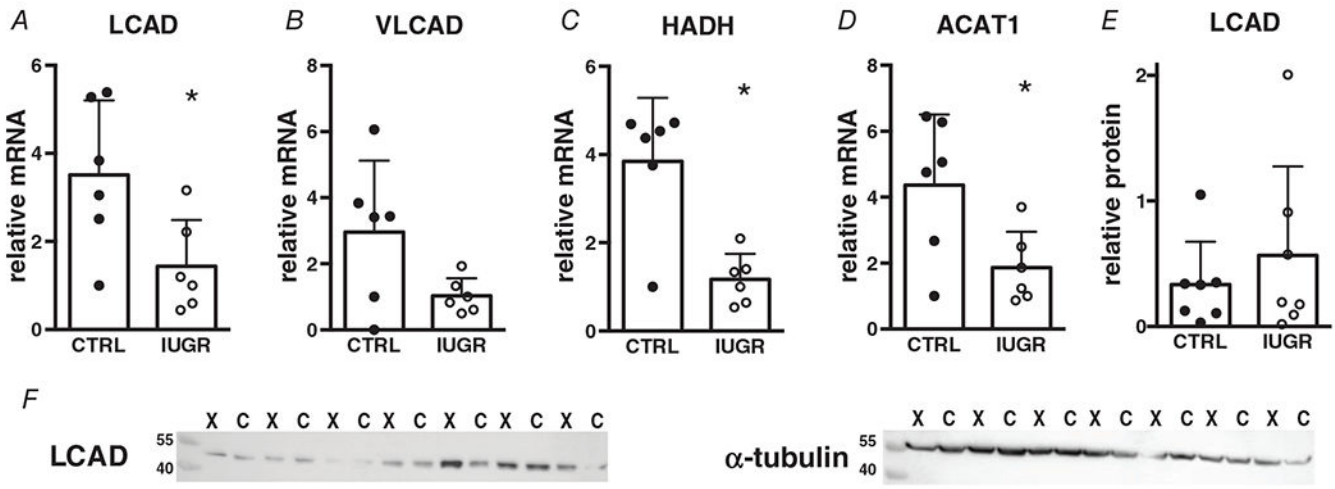

Figure 7. Gene (relative to RPL37a) and protein (relative to alpha-tubulin) expression of mitochondrial β-oxidation enzymes in growth-restricted myocardium

mRNA: $n = 6$ control, $n = 6$ IUGR (LCAD $P = 0.0286$, VLCAD $P = 0.0604$, HADH $P = 0.0017$, ACAT1 $P = 0.0283$) protein: $n = 7$ control, $n = 7$ IUGR (LCAD $P = 0.447$). Means ± SD, $*P < 0.05$. In *F*: C = Control, X = IUGR. Numbers adjacent to ladder represent kDa.

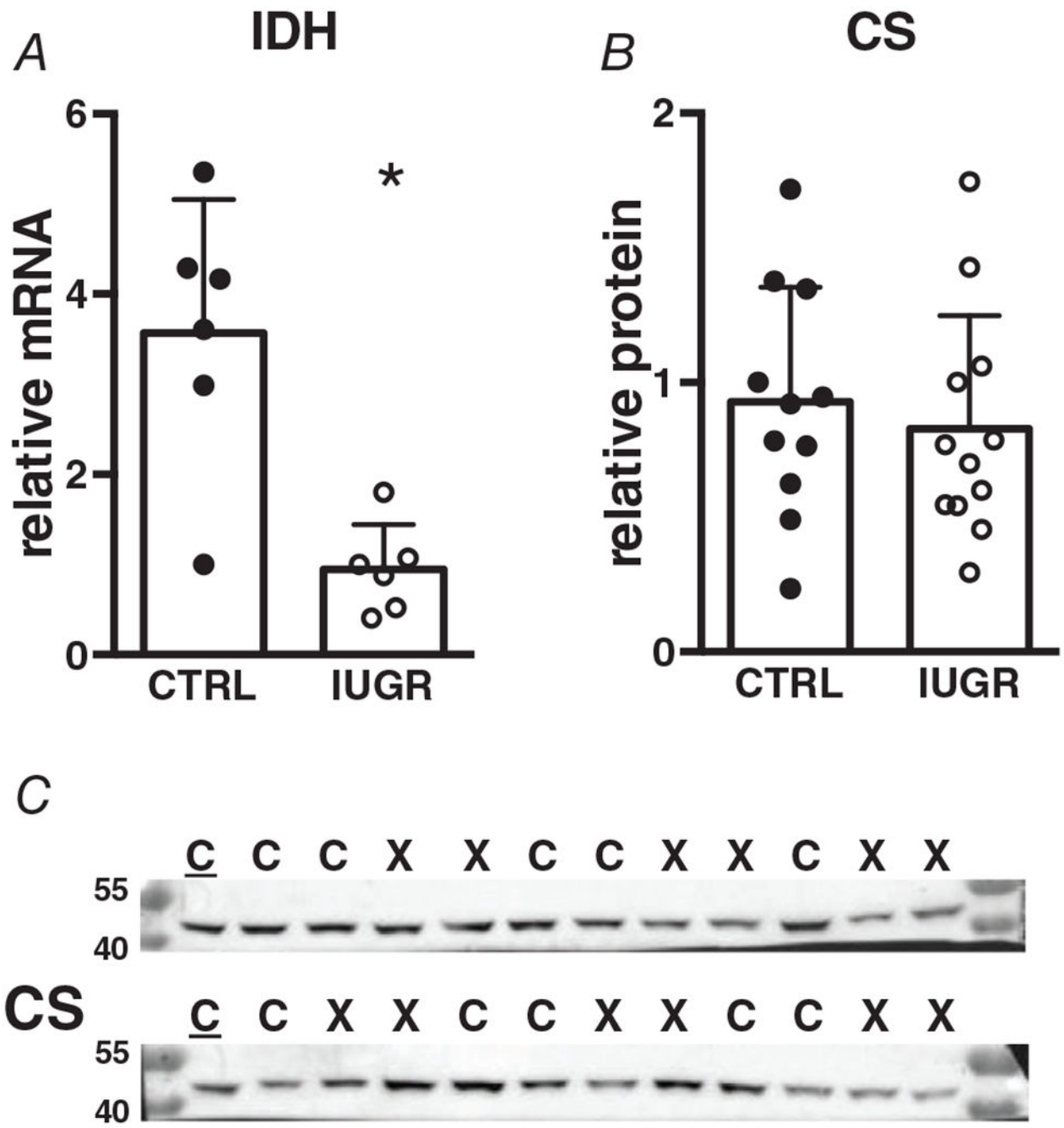

Figure 8. Gene (relative to RPL37a) and protein (relative to total protein) expression of TCA cycle enzymes in growth-restricted myocardium

mRNA: $n = 6$ control, $n = 6$ IUGR (IDH $P = 0.0021$), protein: $n = 11$ control, $n = 12$ IUGR (CS $P = 0.576$). Means ± SD, *$P < 0.05$. In *C*: C = Control, X = IUGR. Numbers adjacent to ladder represent kDa.

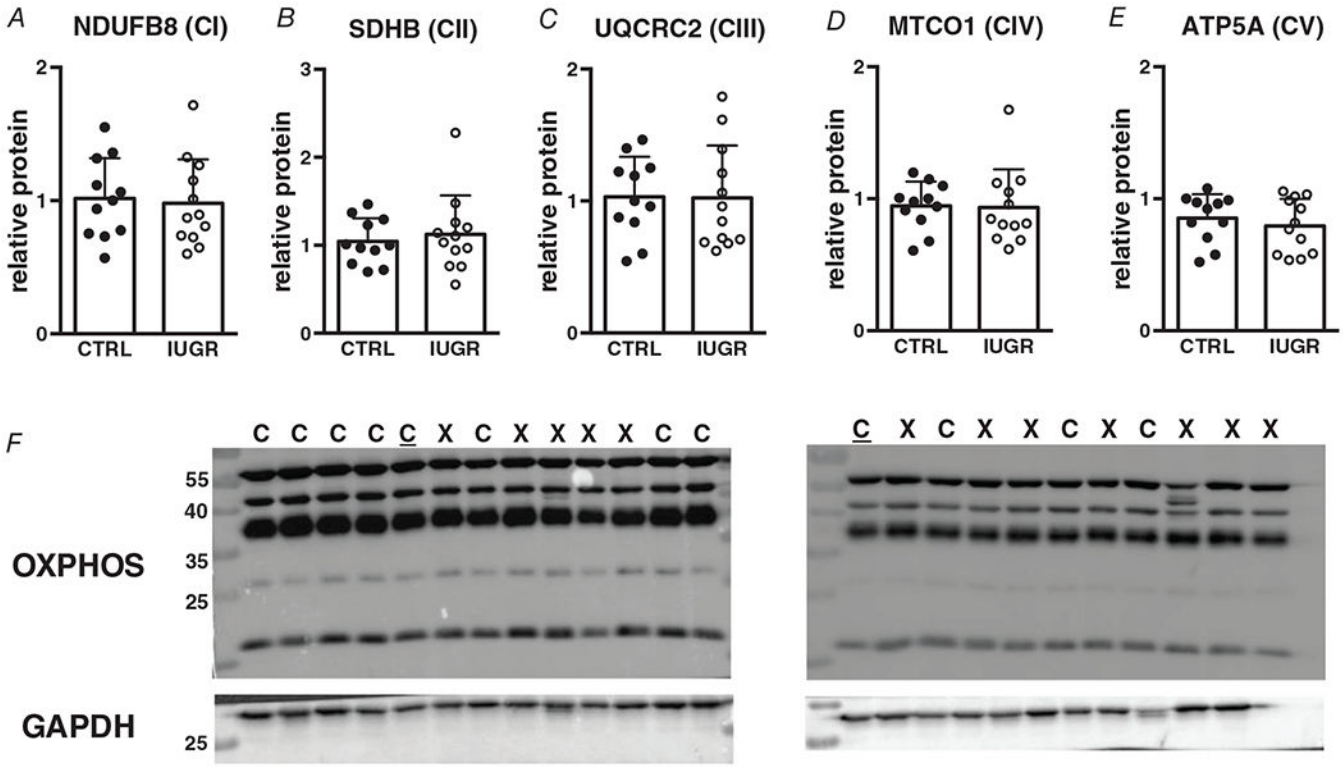

Figure 9. Protein (relative to GAPDH) expression of electron transport chain subunits in growth-restricted myocardium

n = 11 control, *n* = 12 IUGR (NDUFB8 *P* = 0.786, SDHB *P* = 0.609, UQCRC2 *P* = 0.964, MTCO1 *P* = 0.903, ATP5A *P* = 0.487). Means ± SD. In *F*: C = Control, X = IUGR, C = Calibrator Control. Numbers adjacent to ladder represent kDa.

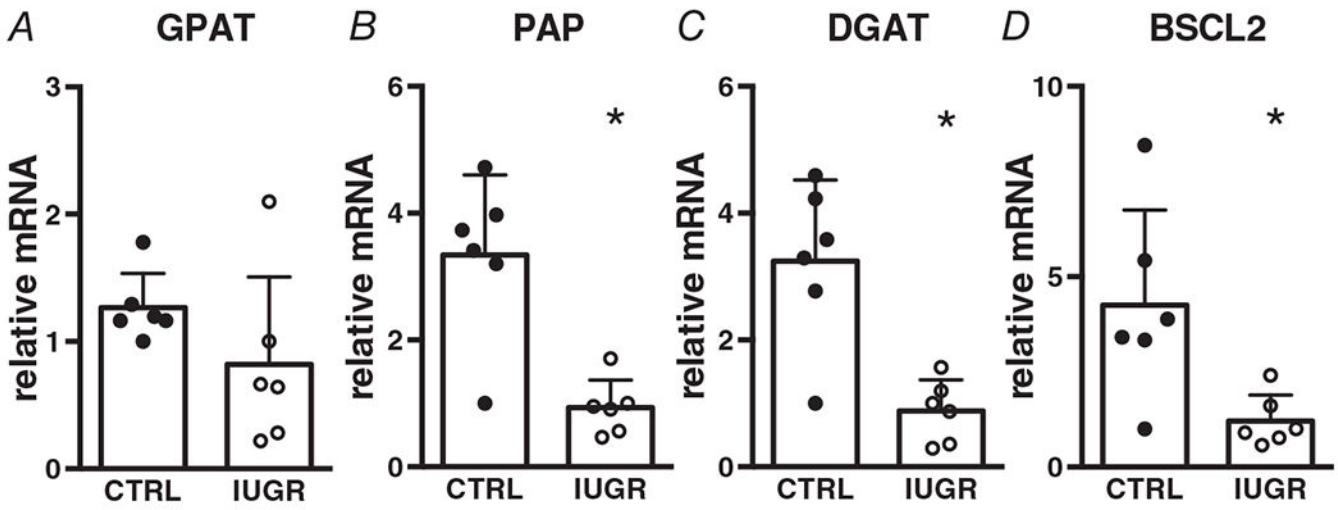

Figure 10. Gene (relative to RPL37a) expression of fatty acid esterification enzymes in growth-restricted myocardium

n = 6 control, n = 6 IUGR (GPAT P = 0.168, PAP P = 0.0013, DGAT P = 0.0018, BSCL2 P = 0.0166). Means ± SD, *P < 0.05.

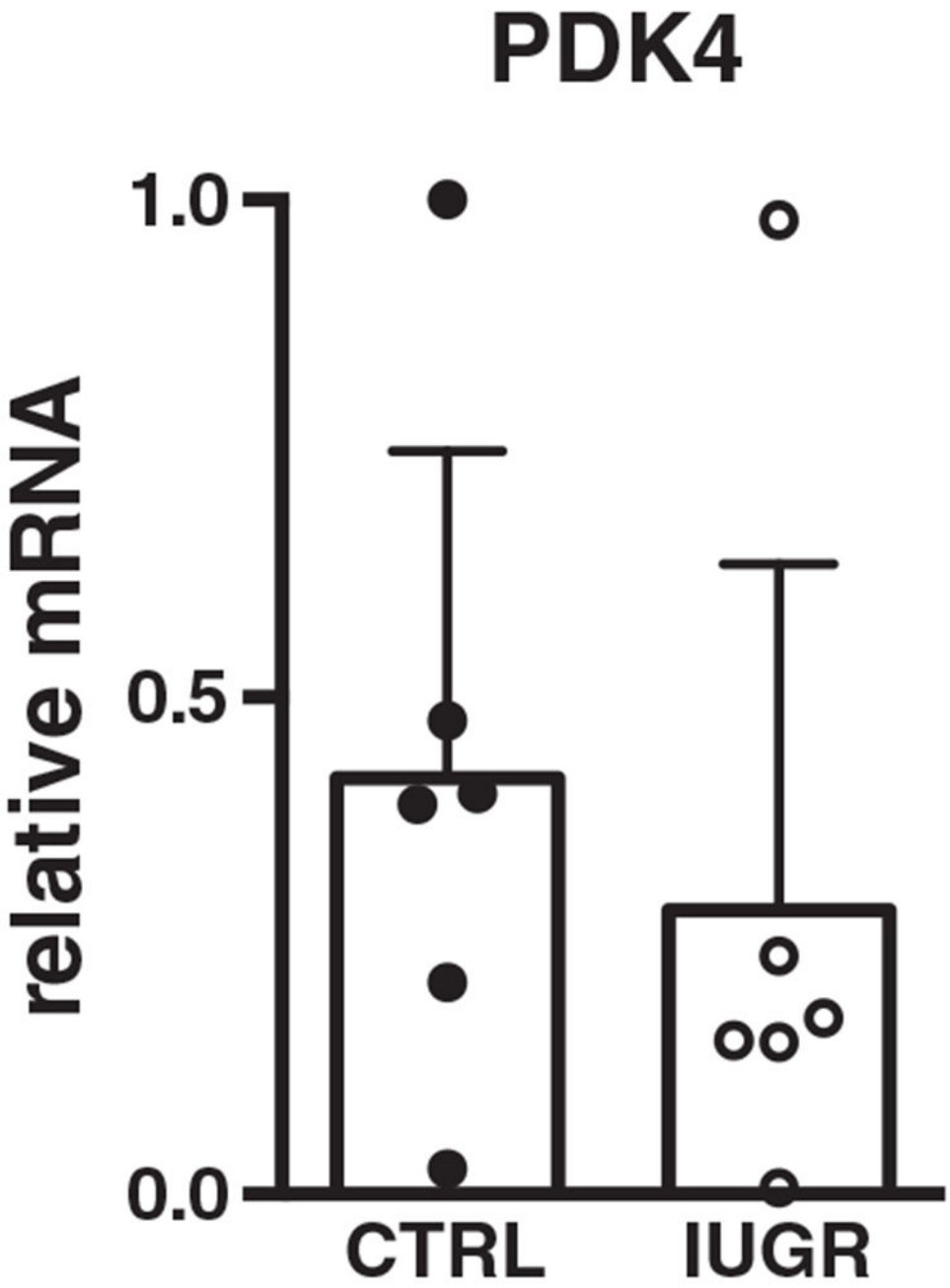

Figure 11. Gene (relative to RPL37a) expression of glycolysis/oxidation regulatory enzyme in growth-restricted myocardium

n = 6 control, n = 6 IUGR (P = 0.511). Mean ± SD.

Table 1.

Sample size and sex distribution

	Plasma acylcarnitines	Lipid droplet imaging	qPCR	Western blotting
Age	126 ± 1 day	125 ± 1 day	126 ± 1 day	126 ± 1 day
Control	*n* = 12 (seven male, five female)	*n* = 12 (eight male, four female)	*n* = 6 (three male, three female)	*n* = 11 (six male, five female)
IUGR	*n* = 12 (five male, seven female)	*n* = 12 (six male, six female)	n = 6 (3 male, 3 female)	*n* = 12 (six male, six female)

IUGR: intrauterine growth-restricted.

Table 2.

Primer sequences

	Sequence 5′–3′		
Gene ID	**Forward**	**Reverse**	**Accession number**
RPL37a (housekeeper)	ACCAAGAAGGTCGGAATCGT	GGCACCACCAGCTACTGTTT	XM_027965159.1
CD36	CTGGTGGAAATGGTCTTGCT	ATGTGCTGCTGCTTATGGGT	XM_027968558.1
FATP6	TTGGAAATGGAGCACGCAGTGA	CTCCCGACTGATCCAATTTTCCCA	KP735933.1
ACSL1	GAGCAGAGGTTCTCAGTGAAGCAA	CGGCTGTCCATCCAGGATTCAATA	XM_015104563.2
ACSL3	GACAGATGCCTTCAAGCTGAAACG	GGAATGGACTCTGCCTCACAGTTT	XM_034955270.1
CPT1	GGATGTTTGAGATGCACGGC	GCCAGCGTCTCCATTCGATA	XM_027965744.1
IDH	CTGTGTTTGAGACGGCTACAAGGA	CGTAGCTGTGGGATTGGCAATGTT	XM_027963525.1
LCAD	TGAAAGCCGCATTGCCATTGAG	ACTTGGATGGCCCGGTCAATAA	XM_004003336.4
VLCAD	AAGATCCCTGAGTGAAGGCCA	TAGAACCAGGATGGGCAGAAA	XM_004012636.3
HADH	AGAAAACCCCAAGGGTGCTGAT	GCCTCTTGAACAGCTCGTTCTT	XM_004009637.4
ACAT1	CTGGGTGCAGGCTTACCTATTTCT	CATAGGGGACATTGGACATGCTCT	XM_027979167.1
GPAT	GAAGTGGCTGGTGAGTTAAACCCT	CAGTCTGATCATTGCCGGTGAAAC	XM_012102930.2
PAP	AGAATGAAGGGAGACTGGGCAAGA	GCAACCAGAGCTCCTTGAATGAGT	XM_004016984.4
DGAT	AGACACTTCTACAAGCCCATGCTC	AGTGCACTGACCTCATGGAAGA	XM_027972747.1
BSCL2	CTGCCTCCCTGACTCTGAAGT	TGCGGAGGCCAGAATGATG	XM_012102049.3
PDK4	CCTGTGATGGATAATTCCCG	TTGGTTCCTTGCTTGGGATA	NM_002612.4

Table 3.

Antibodies used

Protein	Dilution	Catalogue number	Vendor	RRID or reference
CD36	1:1000	133625	abcam	RRID:AB_2716564
ACSL1	1:1000	177958	abcam	(Li et al. 2020)
CPT1a	1:500	12252	Cell Signaling	RRID:AB_2797857
CPT1b	1:1000	22170	ProteinTech	(Abudurexiti et al. 2020)
VDAC	1:1000	12454	Cell Signaling	RRID:AB_2797922
ACADL	1:1000	17526	ProteinTech	(Huang et al. 2014)
CS	1:1000	14309	Cell Signaling	RRID:AB_2665545
OXPHOS cocktail containing: NDUFB8, SDHB, UQCRC2, MTCO1, ATP5A	1:500	110413	abcam	RRID:AB_2629281
GAPDH (housekeeper protein)	1:5000	47339	Novus Biologicals	RRID:AB_10010294
Alpha-tubulin (housekeeper protein)	1:5000	2125	Cell Signaling	RRID:AB_2619646
Anti-rabbit HRP (secondary antibody)	1:5000	7074	Cell Signaling	RRID:AB_2099233
Anti-mouse HRP (secondary antibody)	1:5000	7076	Cell Signaling	RRID:AB_330924